SSC22-WKVI-01

Methodology for Correlating Historical Degradation Data to Radiation-Induced Degradation System Effects in Small Satellites

Richard H. Nederlander, Arthur F. Witulski, Robert A. Reed, Enxia Zhang,
Ronald D. Schrimpf, and Brian D. Sierawski
Department of Electrical Engineering
Vanderbilt University, Nashville, TN 37235 USA; 917-678-4913
richard.h.nederlander@vanderbilt.edu

Gabor Karsai and Nag Mahadevan
Institute for Software Integrated Systems
Vanderbilt University, Nashville, TN 37212 USA

Keivan G. Stassun
Department of Physics and Astronomy
Vanderbilt University, Nashville, TN 37235 USA

Kaitlyn L. Ryder, Rebekah A. Austin, Michael J. Campola, and Ray L. Ladbury
Goddard Space Flight Center (GSFC)
NASA, Greenbelt, MD 20771 USA

ABSTRACT

When constructing a system-level fault tree to demonstrate device-to-system level radiation degradation, reliability engineers need relevant, device-level failure probabilities to incorporate into reliability models. Deriving probabilities from testing can be expensive and time-consuming, especially if the system is complex. This methodology offers an alternative means of deriving device-level failure probabilities. It uses Bayesian analysis to establish links between historical radiation datasets and failure probabilities. A demonstration system for this methodology is provided, which is a TID response of a linear voltage regulator at 100 krad(SiO_2). Data fed into the Bayesian model is derived from literature on the components found within a linear voltage regulator. An example is presented with data pertaining to the device's bipolar junction transistor (BJT)'s gain degradation factor (GDF). Kernel density estimation is used to provide insight into the dataset's general distribution shape. This guides the engineer into picking the appropriate distribution for device-level Bayesian analysis. Failure probabilities generated from the Bayesian analysis are incorporated into a LTspice model to derive a system failure probability (using Monte Carlo) of the regulator's output. In our demonstration system, a 96.5% likelihood of system degradation was found in the assumed environment.

INTRODUCTION

Over the past decade, the number of private companies launching spacecraft into orbit has been exponentially increasing. Specifically, over $258 billion dollars have been invested into 1,688 space organizations globally over the past 10 years [1]. A crucial element to these companies' capabilities is the incorporation of commercial-off-the-shelf (COTS) components into their spacecrafts' system designs. COTS components are electronic parts (e.g., photodiodes, microcontrollers, etc.) that are mass-produced by semiconductor companies and publicly available for purchase. These components tend to be purchased in bulk by companies in industries manufacturing personal electronics (e.g., smartphones, computers, and electric vehicles).

Consequently, COTS part prices are less than for similar devices designed for a spacecraft's mission profile (e.g., radiation-hardened components). Relative to radiation-hardened components, COTS parts tend to be several technological generations more advanced because development is keeping pace with Moore's law [2]. As a result, spacecraft engineers often prefer COTS components over hardened alternatives.

However, COTS parts are not designed for radiation environments because they are built for terrestrial commercial purposes. Even though space radiation (e.g., cosmic rays) can potentially affect terrestrial electronics, these effects are uncommon and not often considered by major purchasers of COTS parts [2][3]. COTS component documentation tends to lack the physical

radiation data necessary for radiation engineers to qualify the parts for a space mission, since terrestrial customers rarely request such information. This lack of awareness of a spacecraft's responses in a radiation environment can pose a risk to the system's reliability. Radiation effects on semiconductors range from recoverable transients observed on current outputs to catastrophic device failure.

As a result, it is important for an engineering team to have a general understanding of their system's failure probability, especially with COTS parts in the system. Deriving such a probability can be difficulty if the spacecraft team lacks an expert who can provide a foundational understanding of potential radiation degradation being introduced into their system. Multiple rounds of radiation testing can also be prohibitive due to test facilities' costs (potentially costing upwards of $1000 per hour), and the time and resources required to design and prepare for testing [3]. Therefore, we propose a method for deriving a preliminary system-level failure probability from component failure data. This method converts device-level failure probabilities derived from historical data of the devices into a system-level failure probability through a Monte Carlo process. A statistical method called kernel density estimation (KDE) informs the engineer of the dataset's distribution shape for individual components for incorporation into the Bayesian model. This process informed us that our selected BJT resulted in the linear voltage regulator having a degradation probability in the selected environment of 96.4%.

BACKGROUND

This paper describes how reliability engineers can use Bayesian analysis to derive failure probabilities from relevant radiation databases (from sources such as the 'parts, materials, and processes encyclopedia' database [4] and the NASA Goddard Space Flight Center's radiation test database [5]). While not a substitute for traditional radiation testing (e.g., MIL-STD-883 1019 for total ionizing dose (TID) effect testing [6]), the methodology in this paper can provide the user with a degree of confidence in the system's reliability. Total ionizing dose is a cumulative, long-term radiation effect that causes gradual performance degradation within semiconductors in response to ionizing particles (e.g., protons or photons) [7]–[9]. This buildup of defects in semiconductors can cause decreased functionality. The following subsections will provide context on the tools used in the methodology.

Bayesian Analysis

Bayesian statistics is guided by Bayes' theorem, which improves knowledge of an event through incremental updates to that initial knowledge of the event [10]. Through this process, the probability of an event's occurrence is continually refined until it no longer fluctuates from the addition of new knowledge. To conduct this analysis, newly obtained failure data (a Posteriori) is added to any initial failure data (a Priori), which is added into a system represented by a Bayesian function. This form of statistical analysis is selected for this methodology because it is ideal for radiation datasets that are small/old/less relevant to the flight system [11]–[13].

The following equations summarize Bayesian analysis:

$$P(A|B) = \frac{P(B|A) * P(A)}{P(B)} \tag{1}$$

$$Posterior = \frac{Likelihood * Prior}{Normalization} \tag{2}$$

In Equation 1, P(A) and P(B) are the independent probabilities of event A and event B. P(A|B) is the probability of A given B. P(B|A) is the probability of B given A. Equation 2 is the qualitative representation of Equation 1. The *posterior* is a probability of an event occurring based on relevant evidence. The *likelihood* is a probability of relevant evidence existing based on an event. The *prior* is also a probability that, in general, is shaped by a probability distribution function (PDF) and assumes an event has happened. The normalization variable in the denominator is a constant determined by the probability of the evidence occurring. After calculating a Posterior probability for a component based on its datasets, it can be incorporated into a fault tree.

Kernel Density Estimation

Kernel density estimation allows engineers to understand the shape of their dataset's distribution so that they can select an appropriate distribution for degradation of a component parameter as a function of ionizing dose. The algorithm can be understood as a systematic means of turning a histogram into a probability density function (PDF) with no prior assumptions as to the overall shape of the PDF. The KDE procedure can also highlight data nuances in the resulting histogram that may not otherwise have been noticed (e.g., bimodal characteristics in the dataset) [14]. Overall, KDE is calculated by weighing the distances of all datapoints within a dataset. Datapoints that are closely packed together results in a higher estimate than if the datapoints were farther apart. Furthermore, the KDE algorithm uses a parameter known as 'bandwidth,' which sets the degree of smoothness for the curve.

$$\hat{f}(x) = \sum_{observations} K\left(\frac{x - observation}{bandwidth}\right) \tag{3}$$

In Equation 3, KDE is represented as taking the sum of all weights of a distance between point x and all other observations in a given dataset. The variable K is the kernel function, and can take the form of a variety of distributions (e.g., normal, lognormal, etc.) [15]. Bandwidth is determined according to a selection optimization model known as 'Scott's Rule' [16]. This model uses a bandwidth factor based on the following equation, where d is the number of dimensions in a probabilistic space and n is the number of datapoints:

$$n^{\frac{-1}{(d+4)}} \tag{4}$$

For unequally weighted points, 'n' is replaced with 'n_{eff}.' n_{eff} is the effective number of datapoints [17]. Meanwhile, the normal distribution is represented as the following:

$$\mathrm{p}(\mathrm{x}|\mu,\sigma^2) = \frac{1}{\sqrt{2\pi\sigma^2}} e^{-\frac{(x-\mu)^2}{2\sigma^2}} \tag{5}$$

And finally, the kernel of the normal distribution is represented as the following:

$$\mathrm{p}(\mathrm{x}|\mu,\sigma^2) \propto e^{-\frac{(x-\mu)^2}{2\sigma^2}} \tag{6}$$

σ^2 is the variance. μ is the mean. It is important to note that the normal distribution is used for the kernel function as an example but is not an assumption of the overall shape of the PDF. In short, KDE is utilized in this work by inputting our dataset's BJT GDFs in a Python package that automatically incorporates the equations mentioned above. An example of KDE applied this research can be found in Fig. 4.

Monte Carlo Method

The Monte Carlo method is a statistical tool that predicts various outcomes within a probabilistic space based on introduced random variables. It is used in this research for calculating a system-level probability of degradation give the that one or more components is degrading because of total ionizing dose. In our case, the probabilistic space is an inverse cumulative distribution (ICDF) for each degraded component based on the probability density distribution of a radiation degradation parameter. The ICDF is then used as a lookup table, which depends on a uniform random number generator [18]. In short, a lookup table maps input values to output values, allowing for the approximation of mathematical functions. The lookup table used in this work can be found in Fig. 1. In short, Monte Carlo helps us infer distributions that approximate system behavior when the system's functionality is unknown. This is distinct from using KDE, which directly estimates a PDF from experimental component data.

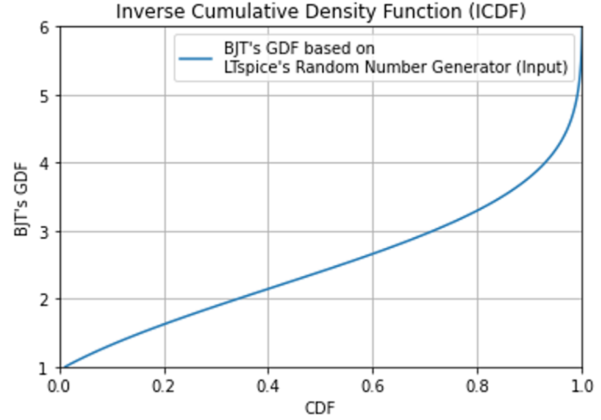

Fig. 1. Lookup table of the BJT's GDF

After incorporating device-level failure probabilities, Monte Carlo analysis can be run through LTspice to output a system-level failure probability. LTspice [19] is a circuit simulator that allows for devices to be analyzed according to user-select component parameters and can be used to simulate radiation effects in integrated circuits at the transistor-level [20][21]. Specifically, an LTspice model is useful for replicating a failure mode on a component to see how it affects the entire circuit. This can be accomplished by adjusting the model parameters of a given components functional model according to observed radiation degradation. The model used in this work can be found in Fig. 2.

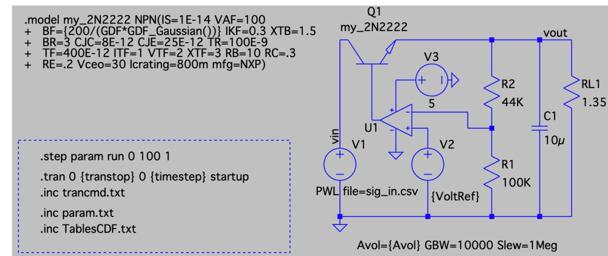

Fig. 2. LTspice schematic of the linear voltage regulator

METHODOLOGY

The methodology can be summarized as follows: device-level data is feed into both KDE and a Bayesian statistical model. The KDE process results in the most likely distribution shape of the dataset, which is then inserted into the Bayesian model so that device-level failure probability distributions can be derived and inputted into a LTspice model of the system. The

LTspice-simulated output of the modeled linear voltage regulator is then run multiple times, and the system-level outputs are converted into a system-level failure probability. This workflow is summarized in Fig. 3.

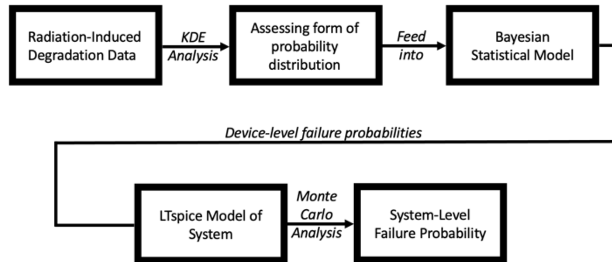

Fig. 3. Workflow of the Methodology

EXPERIMENTAL RESULTS

As a demonstration system for this methodology, a linear voltage regulator is considered with responses to a TID of 100 krad(SiO_2). A linear voltage regulator is an electronic device that maintains a steady voltage. A range of load currents and voltage variations can enter a linear voltage regulator, and a stable DC voltage will be the output [22]. This happens because the regulator adjusts the current flow through the load resistance by comparing the voltage supply's DC output to the regulator's fixed internal reference voltage [23]. Therefore, a linear voltage regulator is useful for regulating the output of an unregulated voltage supply, regardless of load resistance changes. Without a voltage regulator, an unregulated voltage supply can be dangerous for sensitive devices such as digital integrated circuits because current spikes can lead to operating issues such as false triggering, or even destroy the device itself [23]. This can occur because surges within an unregulated voltage supply's input will be expressed in the supply's output.

Results in [22] show that TID affects various devices inside a linear voltage regulator. These TID-sensitive components are the bipolar junction transistor (BJT), the operational amplifier, and the shunt voltage reference. However, the literature and existing datasets show that the regulator's internal BJT is the most sensitive to a TID of 100 krad(SiO_2). As a result, this paper focuses on applying the described methodology to the BJT, although the method is applicable even if all components degrade with TID. Specifically, we focused on using BJT data taken from [12], which contains 19 lots of TID data at doses of 100 krad(SiO_2), 300 krad(SiO_2), and 1 Mrad(SiO_2).

The BJT is a three-terminal device that can control current flow through electrically controlled switches. The npn configuration of the BJT controls larger collector-to-emitter current through relatively smaller input current and positive voltage applied to the base. The 2N222 BJT was selected because its gain degradation factor (GDF) was extensively analyzed in [12]. The BJT itself has a max collector-emitter voltage (V_{CEO}) of 30 V, a max collector-base voltage (V_{CBO}) of 60 V, a max emitter-base voltage (V_{EBO}) of 5 V, and a max collector current (I_C) of 5 A. The gain degradation factor (GDF) is the ratio of pre-rad to post-rad gain at a given dose and test conditions.

A KDE analysis of the 2N2222 BJTs dataset from [12] is shown in Fig. 4. The PDF for a dose of 100 krad(SiO_2) appears to follow a Gaussian distribution, which informs us that a Gaussian distribution should be applied in the Bayesian analysis. The PDFs for 200 and 300 krad(SiO_2) show a departure from Gaussian behavior and more of a multi-modal distribution, so analyses at these dose levels would require a different standard form for the PDF in the MCMC analysis. The two plots in Fig. 5 and Fig. 6 are the Bayesian-derived parameters (mean and standard deviation) of the PDFs. Bayesian statistical modeling packages (e.g., PyMC3 [13], ArviZ [24], and Seaborn [25]) are used to output these failure probability distributions. Both plots assume the data is Gaussian so that the mean of the means (as well as the standard deviation of the means) for possible Gaussian PDFs fit the dataset. Regions of curves that overlap are represented as a shaded region that combines both curves' colors.

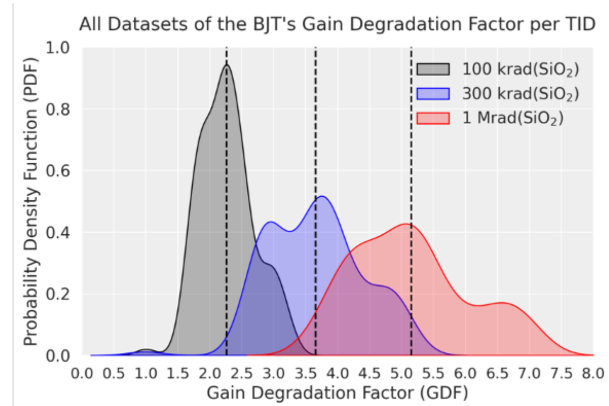

Fig. 4. 3 datasets of GDFs per TID. Dashed black lines represent mean GDF at each TID

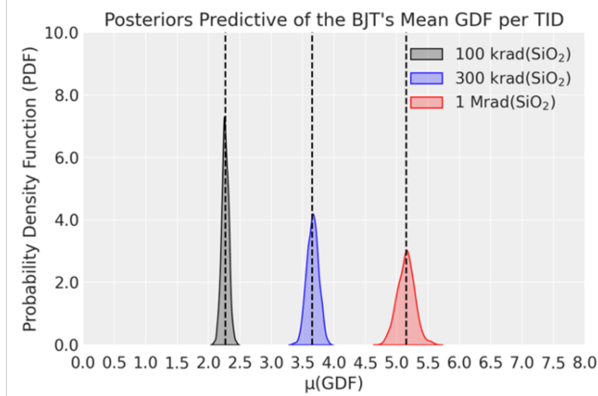

Fig. 5. 3 Bayesian-generated posteriors of mean GDF per TID, plotted as histograms.

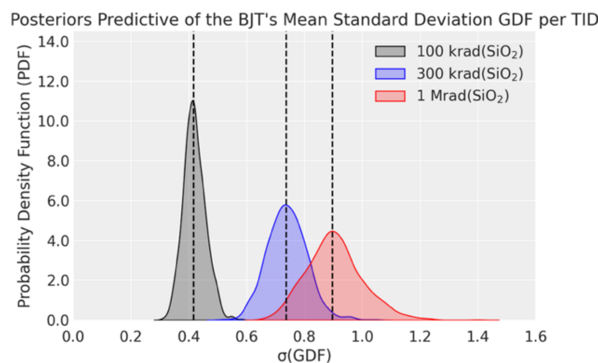

Fig. 6. 3 Bayesian-generated posteriors of standard deviation GDF per TID, plotted as histograms

Simulation Results

The failure probability distribution for the 100 krad(SiO_2) shown in Fig. 5 is sampled and the resultant value of transistor current gain incorporated into the LTspice transistor model (Fig. 2) for voltage regulator simulations in order to observe the output voltage probability distribution. This process is similar to the uncertainty quantification procedure in [26]. The BJT model in LTspice is calibrated by changing the default parameters for the 2N2222. Specifically, its beta is adjusted such that it varies according to a Bayesian fault probability distribution. As mentioned, Monte Carlo can then be applied to the LTspice model to output a degraded voltage probability distribution, as represented in Fig. 7. This process is similar to the uncertainty quantification procedure in [26]. 100 runs in Monte Carlo were conducted such that a different GDF was selected per run based on this Bayesian distribution.

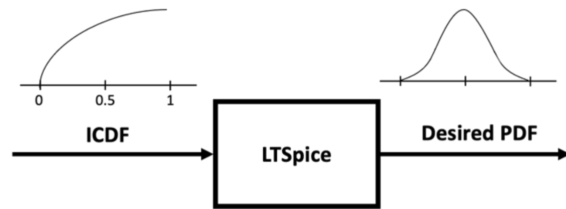

Fig. 7. Image representing LTspice's PDF creation.

The degraded output vs. non-degraded output (and the simulated degraded output's PDF) can be found in Fig. 8. The components' values in LTspice are designed so that the non-degraded output voltage is 1.8 V. In fact, the expected non-degraded output and the average non-degraded simulated output are within a tolerance of 1% of each other (in this case, within 18 mV on either side). Black solid lines in both plots represent the bounds indicative of 1% around 1.8 V.

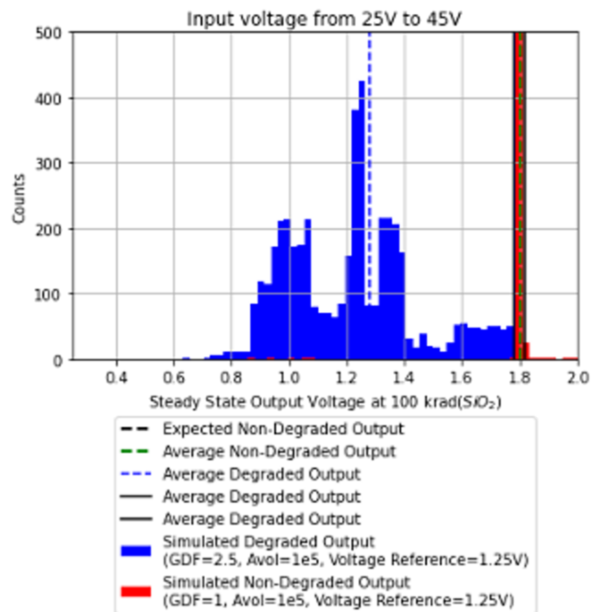

Fig. 8. Degraded vs. Non-degraded output from the LTspice

Discussion

Taking the integral between the two black lines in the Fig. 9 shows that there is approximately a 3.46% likelihood that the system will output that voltage. As a result, there is a 96.54% probability of system degradation. Based on these results, 100 krad(SiO_2) appears to significantly degrade the linear voltage regulator's output voltage. The methodology has now established a correlation between the distribution of the component-level degradation and the distribution of the system-level degradation.

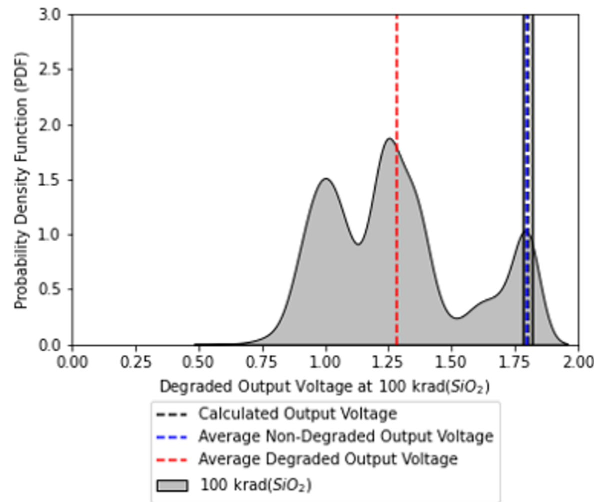

Fig. 9. Degraded vs. Non-degraded output from LTspice, converted into KDE

In this work, a linear voltage regulator's BJT's gain degradation was found to be a significant source of system failure at 100 krad(SiO_2) when not mitigated. This dose level partially represents a radiation environment observed at certain orbits in Earth's geosynchronous orbit (GEO) and Jupiter. Furthermore, this finding can potentially encourage designers to consider spot shielding. Furthermore, this methodology can be generalized to other parts that contain pre-existing radiation degradation datasets. As a result, the procedure described in this study can be used to minimize the amount of radiation testing by serving as an initial screening test. This process can be scaled to incorporate larger systems, such as entire boards. It can also consider other radiation effects such as displacement damage dose (DDD).

CONCLUSION

A novel system-level approach is presented for modeling failure probabilities of radiation vulnerability by using Bayesian analysis to derive probability distributions from physical datasets. By using Bayesian analysis to correlate physical data to failure probabilities, designers at organizations such as universities, startups, and small research laboratories can have an affordable radiation guidance tool. This initial screening process also allows designers to reduce the number of times devices will need to be radiation-tested by highlighting parts with a high risk of failure due to radiation effects, in this case TID. By using historical data and system effects to identify parts that are likely to fail, users can then focus on testing these parts.

By incorporating all possible available data into a Bayesian model, this model can help engineers minimize conventional lot testing and/or radiation-hardened components usage. However, this method does not aim to replace traditional radiation testing (e.g., MIL-STD-883 1019 for total ionizing dose (TID) effect testing [6]), but rather to provide a cost-saving initial screening step that could be useful to budget-constrained organizations (e.g., universities, startups, and small research laboratories).

At the moment, one potential issue is finding radiation datasets of components that all share the same total ionizing dose levels. For example, the BJT has been analyzed at 100 krad(SiO_2) but raw data found so far for the error amplifier and shunt voltage reference do not reach that TID magnitude. After review, this issue can be resolved by shifting the focus toward the impact of degradation effects and away from the ionizing dose levels. As a result, dose levels will be a non-significant variable.

Acknowledgements

This work is supported by the NASA Grant No. 80NSSC20K0424.

References

[1] "Space Investment Quarterly: Q1 2022," Space Capital, Quarterly Report, Mar. 2022. [Online]. Available: https://www.spacecapital.com/quarterly

[2] D. M. Fleetwood, "Evolution of Total Ionizing Dose Effects in MOS Devices With Moore's Law Scaling," *IEEE Trans. Nucl. Sci.*, vol. 65, no. 8, pp. 1465–1481, Aug. 2018.

[3] K. A. LaBel, "A Technical and Cost Perspective on Radiation Testing Challenges," presented at the Microelectronics Reliability and Qualification Workshop, Los Angeles, CA, Dec. 04, 2006. [Online]. Available: https://radhome.gsfc.nasa.gov/radhome/papers/MRQW06_LaBel.pdf

[4] "PMPedia - Parts, materials, and processes encyclopedia," *PMPedia*, 2021. https://pmpedia.space/ (accessed Aug. 20, 2021).

[5] "GSFC Radiation Data Base," *Radiation Effects & Analysis*, Dec. 01, 2021. https://radhome.gsfc.nasa.gov/radhome/RadDataBase/RadDataBase.html (accessed Dec. 01, 2021).

[6] Department of Defense, "MIL-STD-883 test method 1019.7 ionizing radiation (total dose) test procedure," *Test Method Standard Micro-circuits*, Sep. 30, 2010.

[7] M. R. Shaneyfelt, J. R. Schwank, P. E. Dodd, and J. A. Felix, “Total Ionizing Dose and Single Event Effects Hardness Assurance Qualification Issues for Microelectronics,” *IEEE Trans. Nucl. Sci.*, vol. 55, no. 4, pp. 1926–1946, Aug. 2008.

[8] D. M. Fleetwood and H. A. Eisen, “Total-dose radiation hardness assurance,” *IEEE Trans. Nucl. Sci.*, vol. 50, no. 3, pp. 552–564, Jun. 2003.

[9] “Ionizing dose and neutron hardness assurance guidelines for microcircuits and semiconductor devices,” Naval Publications and Form Center (NPFC), Standards MIL-HDBK-814, 1994. [Online]. Available: https://standards.globalspec.com/std/490578/mil-hdbk-814

[10] H. Stark and J. Woods, *Probability, Statistics, and Random Processes for Engineers*, 4th ed. Boston: Pearson, 2011.

[11] K. Kruckmeyer, T. Trinh, L. McGee, and A. T. Kelly, “Impact of reference voltage on the ELDRS characteristics of the LM4050 shunt voltage reference,” in *Proc. 12th Eur. Conf. Radiat. Effects Compon. Syst.*, Sep. 2011, pp. 926–930.

[12] R. Ladbury and B. Triggs, “A Bayesian Approach for Total Ionizing Dose Hardness Assurance,” *IEEE Trans. Nucl. Sci.*, vol. 58, no. 6, pp. 3004–3010, Dec. 2011.

[13] J. Salvatier, T. V. Wiecki, and C. Fonnesbeck, “Probabilistic programming in Python using PyMC3,” *PeerJ Comput. Sci.*, vol. 2, p. e55, Apr. 2016.

[14] M. J. Campola, M. C. Casey, E. P. Wilcox, C. Seidleck, and A. M. Phan, “Discrete Binning Analysis of Single Event Transient Pulse Width for Rate Calculations,” Oct. 06, 2020. Accessed: May 06, 2022. [Online]. Available: https://ntrs.nasa.gov/citations/20205007782

[15] M. Conlen, “Kernel Density Estimation,” *Mathisonian*, Dec. 27, 2018. https://mathisonian.github.io/kde/ (accessed Nov. 03, 2021).

[16] D. M. Bashtannyk and R. J. Hyndman, “Bandwidth selection for kernel conditional density estimation,” *Comput. Stat. Data Anal.*, vol. 36, no. 3, pp. 279–298, May 2001.

[17] M. Brett, “An introduction to smoothing — Tutorials on imaging, computing and mathematics,” *Tutorials on imaging, computing and mathematics*, Oct. 26, 2014. https://matthew-brett.github.io/teaching/smoothing_intro.html (accessed Oct. 17, 2021).

[18] R. Faehnrich, “Spice Simulates Custom Random Distributions for Monte Carlo Analysis,” *Electronic Design*, Feb. 04, 2019. https://www.electronicdesign.com/technologies/test-measurement/article/21807539/spice-simulates-custom-random-distributions-for-monte-carlo-analysis (accessed Oct. 29, 2021).

[19] Analog Devices, “LTspice Simulator | Analog Devices,” *Analog Devices*, 2021. https://www.analog.com/en/design-center/design-tools-and-calculators/ltspice-simulator.html (accessed Sep. 28, 2021).

[20] C. T. Kleiner and G. C. Messenger, “An Improved Bipolar Junction Transistor Model for Electrical and Radiation Effects,” *IEEE Trans. Nucl. Sci.*, vol. 29, no. 6, pp. 1569–1579, Dec. 1982.

[21] X. Huang, A. M. Francis, A. B. Lostetter, and H. A. Mantooth, “Compact modeling of environmentally induced radiation effects on electrical devices,” in *IEEE Aerosp. Conf. Proc. (IEEE Cat. No.04TH8720)*, Mar. 2004, vol. 4, pp. 2597–2607. doi: 10.1109/AERO.2004.1368054.

[22] A. T. Kelly, P. C. Adell, A. F. Witulski, W. T. Holman, R. D. Schrimpf, and V. Pouget, “Total Dose and Single Event Transients in Linear Voltage Regulators,” *IEEE Trans. Nucl. Sci.*, vol. 54, no. 4, pp. 1327–1334, Aug. 2007.

[23] P. Scherz and S. Monk, *Practical Electronics for Inventors, Fourth Edition*, 4th ed. New York: McGraw-Hill Education, 2016. Accessed: Oct. 01, 2021. [Online]. Available: https://www.accessengineeringlibrary.com/content/book/9781259587542

[24] R. Kumar, C. Carroll, A. Hartikainen, and O. Martin, “ArviZ a unified library for exploratory analysis of Bayesian models in Python,” *JOSS*, vol. 4, no. 33, p. 1143, Jan. 2019.

[25] M. L. Waskom, “seaborn: statistical data visualization,” *J. Open Source Softw.*, vol. 6, no. 60, p. 3021, 2021, doi: 10.21105/joss.03021.

[26] G. Karsai *et al.*, “System-Level Uncertainty Quantification from Component-level Radiation Effects,” presented at the Proc. 21st Eur. Conf. Radiat. Effects Compon. Syst., Sep. 2021.